Journal of Medicinal Chemistry Article

J. Med. Chem. **2010,** *53,* 2589–2600 **2589**
DOI: 10.1021/jm100025u

A New Class of Naphthalimide-Based Antitumor Agents That Inhibit Topoisomerase II and Induce Lysosomal Membrane Permeabilization and Apoptosis

Zhuo Chen,[†] Xin Liang,[†] Huanying Zhang,[†] Hua Xie,[†,‡] Jianwen Liu,[†] Yufang Xu,*[,†] Weiping Zhu,[†] Yi Wang,[‡] Xin Wang,[†] Shaoying Tan,[†] Dong Kuang,[†] and Xuhong Qian*[,†]

[†]*State Key Laboratory of Bioreactor Engineering, Shanghai Key Laboratory of Chemical Biology, School of Pharmacy, East China University of Science and Technology, Shanghai 200237, China, and* [‡]*Division of Anti-tumor Pharmacology, State Key Laboratory of Drug Research, Shanghai Institute of Materia Medica, Chinese Academy of Sciences, Shanghai 201203, China*

Received January 10, 2010

Based on the advantages of multitarget drugs for cancer treatment, a new class of naphthalimides was designed, synthesized, and proved to inhibit topoisomerase II (topo II), induced lysosomal membrane permeabilization (LMP), and ultimately caused apoptosis and cell death. The majority of compounds **7a**−**d** and **8a**−**d** potently inhibited the growth of the five tested cancer cell lines with IC_{50} values ranging from 2 to 10 μM and are more active than amonafide, a naphthalimide that was in phase III clinical trials. These compounds were tested for their interactions with DNA and their cell-free topo II inhibition activities, which demonstrated these compounds were weak DNA binders but modest topo II inhibitors. Furthermore, compounds **7b**−**d** were found to notably induce LMP and exhibited better antiproliferative activity compared with their single-target analogues. All of the newly synthesized compounds were demonstrated to efficiently induce apoptosis via a mitochondrial pathway. Accordingly, a new paradigm was suggested for the design of novel multitarget anticancer drugs.

Introduction

Target cancer therapy interfering with a single biological molecule or pathway has been successfully utilized in the clinic.[1−3] It exhibits identified pharmacological effects to a specific molecular target or pathway and may minimize the risk of side effects.[4−6] However, cancer is a complex disease with redundant and robust biological networks. In many cases, when a specific biological target or pathway is completely inhibited, cancer cells can find "backup" systems to compensate the change, which greatly compromises the efficacy. There is general belief that agents modulating more than one target should have superior efficacy compared to single target drugs.[7−11] Modulating multiple targets simultaneously can be achieved by the combination of multiple drugs with different mechanisms or by single chemical entity that could modulate several targets of a multifactorial disease. Although combinational therapy has been successfully used for cancer treatment in the clinic, it usually exhibits complex pharmacokinetic and pharmacodynamic relationships and toxicology profiles.[12−14] Consequently, there are increasing interests in discovering agents that simultaneously address more than one biological target for cancer treatment.[15−17]

Apoptosis is a fundamental process in normal development and tissue homeostasis of multicellular organisms. It is characterized by DNA fragmentation, chromatin condensation, cell shrinkage, and membrane blebbing.[18] Malfunction of apoptosis, especially excessive inhibition of apoptosis, contributes to tumorigenesis, tumor progression, and therapy resistance.[19−21] There are two major apoptotic pathways: the extrinsic pathway triggered by the activation of death receptors and the intrinsic mitochondrial pathway in which mitochondrial outer membrane permeabilization (MOMP)[a] plays a crucial role.[22,23] The induction of apoptosis is considered to be one of the most appropriate ways for cancer therapy and may facilitate eliminating neoplastic cells permanently.[19,24,25]

Lysosomes are highly dynamic intracellular organelles that involve with the biosynthetic, endocytic, and autophagic pathways.[26,27] They control the recycling of the majority of cellular macromolecules and organelles through more than 50 acid hydrolases. Cathepsin proteases are the most well studied lysosomal hydrolases and overexpressed in the tumor environment. It has been demonstrated that in murine cancer models cathepsins enhance cancer progression by stimulating angiogenesis, tumor growth, and invasion when they are outside the tumor cells.[28] On the other hand, LMP releases cathepsins into the cytosol and thereby triggers either necrotic or apoptotic cell death pathways. LMP not only triggers the MOMP-mediated intrinsic apoptosis pathway as a result of the activation of the proapoptotic Bcl-2 family of proteins by cathepsins.[26] More importantly, cytosolic cathepsins can also trigger caspase- and mitochondrion-independent programmed cell death even in highly resistant cancer cells with multiple defects in the classic apoptosis pathway.[29]

*Corresponding author. E-mail: yfxu@ecust.edu.cn; xhqian@ecust.edu.cn. Tel: 86-21-64251399. Fax: 86-21-64252603.

[a]Abbreviations: AO, acridine orange; CD, circular dichroism; CT DNA, calf thymus DNA; DDQ, 2,3-dichloro-5,6-dicyanobenzoquinone; EB, ethidium bromide; FITC, fluorescein isothiocyanate; kDNA, kinetoplast DNA; LMP, lysosomal membrane permeabilization; MOMP, mitochondrial outer membrane permeabilization; MSDH, *O*-methylserine dodecylamide hydrochloride; PI, propidium iodide; PS, phosphatidylserine; TLC, thin-layer chromatography; topo II, topoisomerase II.

Published on Web 02/19/2010

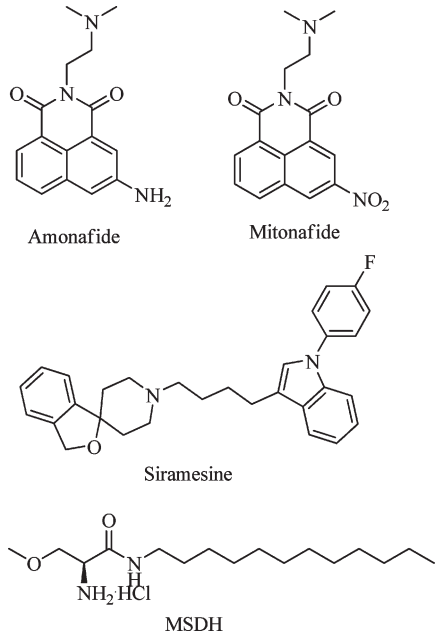

Figure 1. Chemical structures of amonafide, mitonafide, siramesine, and MSDH.

Tumor cells may be preferentially sensitive to agents that trigger the lysosomal apoptosis pathway, suggesting that a reasonable therapeutic window could be achieved for the LMP-inducing agents.[30] Thus, LMP-inducing agents have great potential to be developed as novel cancer therapy.[31−33] Lysosomotropic detergents are highly lipophilic weak bases containing straight-chain hydrocarbon "tails".[34] Some lysosomotropic detergents are well-known LMP inducers, exemplified by siramesine and *O*-methylserine dodecylamide hydrochloride (MSDH) (Figure 1).[35−37] Siramesine possesses potent anticancer activity both *in vitro* and *in vivo* and is in preclinical development.[34,38] It accumulates in lysosomes and destabilizes them, inducing lysosomal leakage and cathepsin-dependent death of cancer cells even in the presence of the prosurvival Bcl-2 family of proteins.[36,38]

DNA-damaging agents constitute a cornerstone of cancer therapy and contribute to the survival of cancer patients in combination with drugs of different mechanisms of action. However, the severe toxicity and drug resistance in the clinic is the Achilles' heel of DNA-damaging agents.[39,40] By targeting DNA-associated processes, enhanced selectivity for cancer cells could be acquired. For example, naphthalimides are an important class of DNA intercalators and have been demonstrated to inhibit topo II.[41,42] Amonafide and mitonafide (Figure 1) were two of the most active naphthalimide-based topo II inhibitors and had been tested in clinical trials. On account of central neurotoxicity and limited efficacy in solid tumors, the clinical development was regrettably terminated.[41,43] To improve the efficacy and the toxicological profiles, considerable efforts have been attempted on the design of more active naphthalimides,[44−47] but most of the efforts were only focused on the analogues with higher DNA-binding affinity.[48]

We report herein a new class of naphthalimides that have the structural features of both DNA intercalators and lysosomotropic detergents. The naphthalimide core was functionalized at the 2- and 6-positons with polyamines and long alkyl chains. The elimination of the amino group at the 5-position would avoid the amino acetylation that caused unpredictable toxicity of amonafide.[49] We demonstrated that these new naphthalimides inhibited topo II, induced LMP and apoptosis, and thereby exhibited much more potent antiproliferative activity than amonafide.

Results and Discussion

Chemistry. The synthesis of the target compounds was shown in Scheme 1. Naphthalimide derivatives **7a**−**d** and **8a**−**d** containing polyamines and long hydrocarbon chains were prepared in a facile four-step sequence in high yield. The commercially available 6-bromobenzo[*de*]isochromene-1,3-dione was condensed with 3-aminopropan-1-ol to afford **1a**. The bromine at the 6-position of **1a** was readily displaced with octan-1-amine under Ullmann's condition to give **3a**. This alcohol was converted into the corresponding bromide **5a** using a system of Ph_3P/2,3-dichloro-5,6-dicyanobenzoquinone (DDQ) and tetrabutylammonium bromide in high yield.[50] This bromination was also attempted using PBr_3 as brominating agent, but **5a** was obtained in much lower yield. Finally, the alkylation between **5a** and 1-methylpiperazine was accomplished in chloroform with high selectivity to provide the target compound **7a**. As shown in Scheme 1, compounds **7b**−**d** and **8a**−**d** were prepared by following similar sequences for the synthesis of **7a**.

Compounds **10a**−**d** were prepared as reference compounds to highlight the importance of polyamines and long alkyl chains to the cytotoxicity. **10d** and **10b** were monoamine analogues of compounds **7a**−**d** and **8a**−**d**; **10a** and **10c** contained only either long alkyl chains or a basic side chain. **10a** and **10b** were obtained by the amination of intermediate **2b** with 1-octanamine and *N*′,*N*′-dimethylethane-1,2-diamine, respectively. Similarly, compounds **10c** and **10d** were synthesized. It is worth mentioning that, in the synthesis of **10c**, $CuSO_4$ was added as a catalyst to decrease the reaction temperature so that the low boiling point methylamine aqueous solution could be used.[51]

***In Vitro* Cytotoxic Activity.** The antiproliferative activities of compounds **7a**−**d**, **8a**−**d**, and **10a**−**d** were evaluated in five human cancer cell lines: HeLa (human cervical carcinoma cell line), HL-60 (human promyelocytic leukemia cell line), MCF-7 (human caucasian breast adenocarcinoma cell line), MKN45 (human gastric cancer cell line), and LS174 (human colon adenocarcinoma cell line). Amonafide was tested as a reference compound. As shown in Table 1, most of the compounds displayed significant antitumor activities with IC_{50} values of low single digital to double digital micromolar. All compounds except **10a** and **10c** exhibited better cytotoxic activity than amonafide in the tested cancer cell lines, which strongly argued for the rationale of the design. Moreover, the introduction of polyamines in **7a**−**d** and **8a**−**d** reduced cell proliferation more significantly in the majority of these five cell lines than their monoamine precursors **10b** and **10d**. Interestingly, compounds **7a**−**d** with the polyamine groups at the 2-position inhibited the growth of the cancer cells better than their counterparts **8a**−**d** with the same polyamine group at the 6-position. Finally, it was found that the flexibility of polyamine and the length of the alkyl chain significantly affected the cytotoxic activity (e.g., **7a** vs **7c**, **7b** vs **7d**).

DNA Intercalating Studies by Circular Dichroism (CD) Spectra. Since DNA is usually considered to be the main target for naphthalimide derivatives, compounds **7a**−**d** and **8a**−**d** were tested for their interaction with DNA. Drug-induced calf

Scheme 1[a]

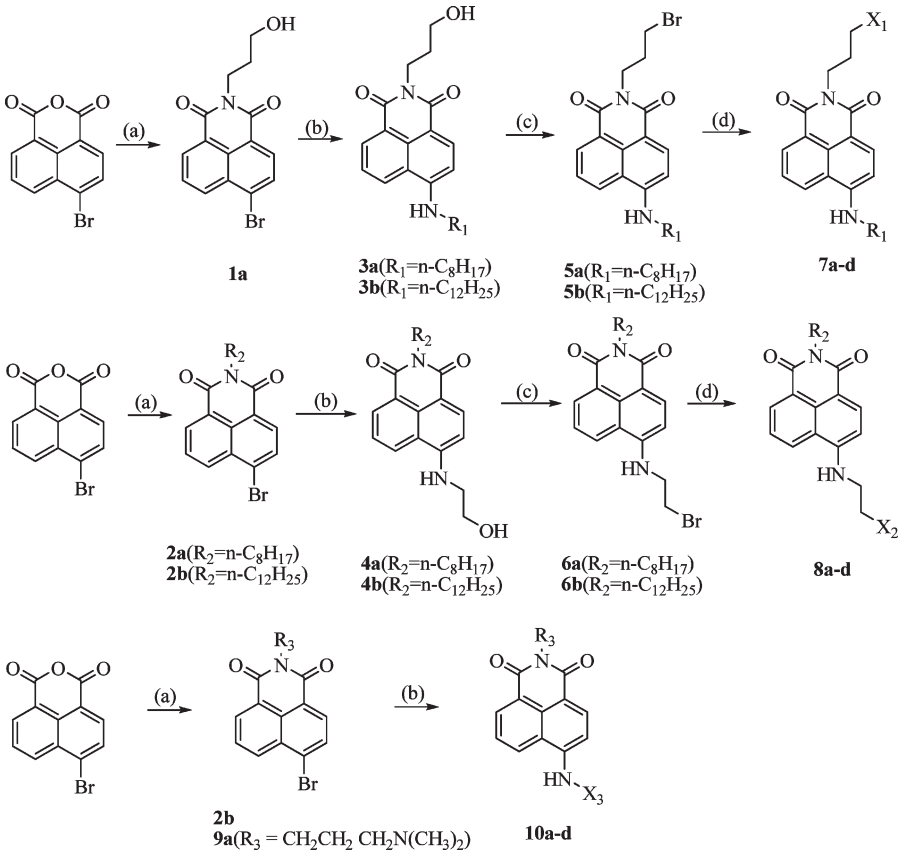

[a] Reagents: (a) 1.1 equiv of corresponding primary amines, ethanol, reflux, 85−95%; (b) 3.0 equiv of corresponding primary amines, 2-methoxyethanol, reflux, 82−90% (for **10c**, 40% methylamine aqueous solution, 2.5 equiv of $CuSO_4$, reflux, 86%); (c) 1.2 equiv of DDQ, 1.2 equiv of PPh_3, 1.2 equiv of $(n\text{-butyl})_4NBr$, CH_2Cl_2, room temperature, 72−82%; (d) 5.0 equiv of corresponding polyamines, 1.2 equiv of KI, $CHCl_3$, reflux, 60−85%.

thymus DNA (CT DNA) conformational changes are analyzed using CD spectroscopy, which exhibit a negative peak around 245 nm as a result of the helical B conformation and a positive peak around 275 nm due to base stacking.[52,53] As shown in Figure 2, amonafide, as a well-known DNA intercalator, led to a decrease of the negative peak and an increase of the positive peak. In contrast with amonafide, compounds **7a**−**d** and **8a**−**d** did not cause any appreciable change in the CD spectra of CT DNA, suggesting that these compounds were weaker DNA intercalators.

Fluorescent Spectra Studies. To further investigate the interactions of these new naphthalimides with DNA, the fluorescence quenching technique was employed to measure the Scatchard binding constants (K_b) for amonafide and a representative naphthalimide **8c**. As shown in Figure 3, the apparent binding constant (K_b) to CT DNA was determined to be 1.43×10^5 M^{-1} for amonafide. However, a positive Scatchard binding constant could not be obtained for **8c**. These results clearly indicated that compound **8c** could not intercalate into DNA as amonafide. This is consistent with the results obtained from the CD spectra experiments.

DNA Relaxation Assay. To investigate if these naphthalimides could cause any conformational changes of DNA, we performed the gel electrophoresis of pBR322 plasmid DNA after incubation with the naphthalimides. It is well documented that DNA of different conformation would migrate on the gel at a different rate.[54] As shown in Figure 4, the DNA in the supercoiled circular form was completely relaxed by the DNA intercalator doxorubicin (lane 7), and no pronounced DNA relaxation was observed for amonafide, **7a**−**d**, and **8a**−**d**.

Topo II Inhibition Assay. Topo II, an important nuclear enzyme, is involved in the process of DNA breakage/reunion by catalyzing DNA unwinding for transcription, replication, recombination, chromosome condensation, and decondensation through the formation of an intermediate called the "cleavable complex".[55−57] Naphthalimides poison topo II by forming and stabilizing a ternary drug−DNA−topoisomerase complex.[41,58] The kinetoplast DNA (kDNA) decatenation assay has been utilized to test drug potential to inhibit topo II activity in a cell-free system, as topo II can catalyze the decatenation of kDNA in the presence of ATP.[59] As shown in Figure 5, all of the tested compounds could reduce the kDNA minicircles, suggesting that they were able to inhibit topo II activity. In particular, compounds **8c**,**d** showed similar poisoning potency to topo II as amonafide. It was worth noting that the flexible and linear polyamine analogues (**8c**, **8d**) exhibited stronger topo II inhibition activity than their half-rigid polyamine analogues (**8a**, **8b**), which was well consistent with the antiproliferative activity in the cell-based assay.

LMP Induction. The induction of LMP by the new naphthalimides was analyzed using the lysosomotropic weak base acridine orange (AO), which prefers to accumulate in normal lysosomes.[26] AO is a metachromatic fluorophore turning red in lysosomes after excitation with blue light. LMP results in the relocation of AO from lysosomes to

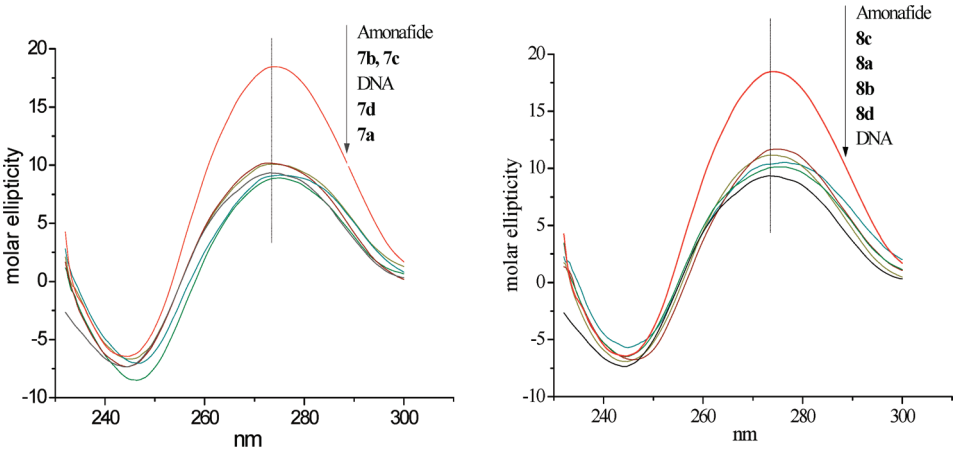

Figure 2. CD spectra of CT DNA (100 μM) incubated with target compounds (20 μM).

Table 1. Structure−Activity Relationship of the Target Compounds and Amonafide

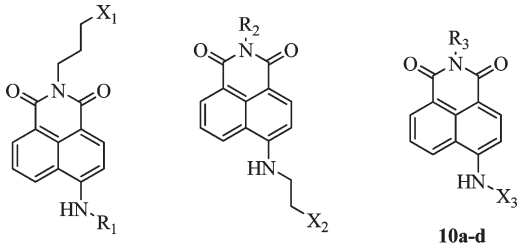

7a-d **8a-d** **10a-d**

Compound	R, X =	Cytotoxicity (IC_{50}, μM)				
		HL-60	HeLa	MCF-7	LS174	MKN45
7a	R_1=n-C_8H_{17}, X_1= 	5.70	8.10	5.72	18.39	22.16
7b	R_1=n-$C_{12}H_{25}$,X_1= 	2.98	2.89	2.48	7.43	8.43
7c	R_1=n-C_8H_{17}, X_1= 	2.67	4.06	2.41	9.16	14.75
7d	R_1=n-$C_{12}H_{25}$, X_1= 	4.04	4.71	2.56	9.43	15.48
8a	R_2=n-C_8H_{17}, X_2= 	12.02	7.90	8.35	17.90	17.42
8b	R_2=n-$C_{12}H_{25}$, X_2= 	7.05	5.45	2.79	12.67	9.28
8c	R_2=n-C_8H_{17}, X_2= 	5.13	4.5	3.76	9.27	9.28
8d	R_2=n-$C_{12}H_{25}$, X_2= 	6.63	16.84	4.52	18.60	11.83
10a	R_3=n-$C_{12}H_{25}$, X_3=n-C_8H_{17}	>50	46.43	>50	>50	>50
10b	R_3=n-$C_{12}H_{25}$, X_3= $(CH_2)_2$ $N(CH_3)_2$	5.32	9.13	3.57	12.78	9.03
10c	R_3= $(CH_2)_3N(CH_3)_2$, X_3= CH_3	21.61	23.37	9.66	31.48	>50
10d	R_3= $(CH_2)_3N(CH_3)_2$, X_3= n-C_8H_{17}	5.53	8.52	5.15	5.87	17.55
Amonofide		17.96	10.67	11.88	20.28	>50

cytosol, and the fluorescence changes from red to green. Thus, red fluorescence assaying (AO uptake method) was used here to evaluate pronounced lysosomal rupture.[60−62] The LMP induction was measured at three different concentrations of these compounds. As shown in Figure 6, compounds **7b−d** induced considerable decreases in the amount of cells with normal AO red fluorescence, indicating significant LMP. The LMP induced by compounds **7b−d** was dose-dependent, and the

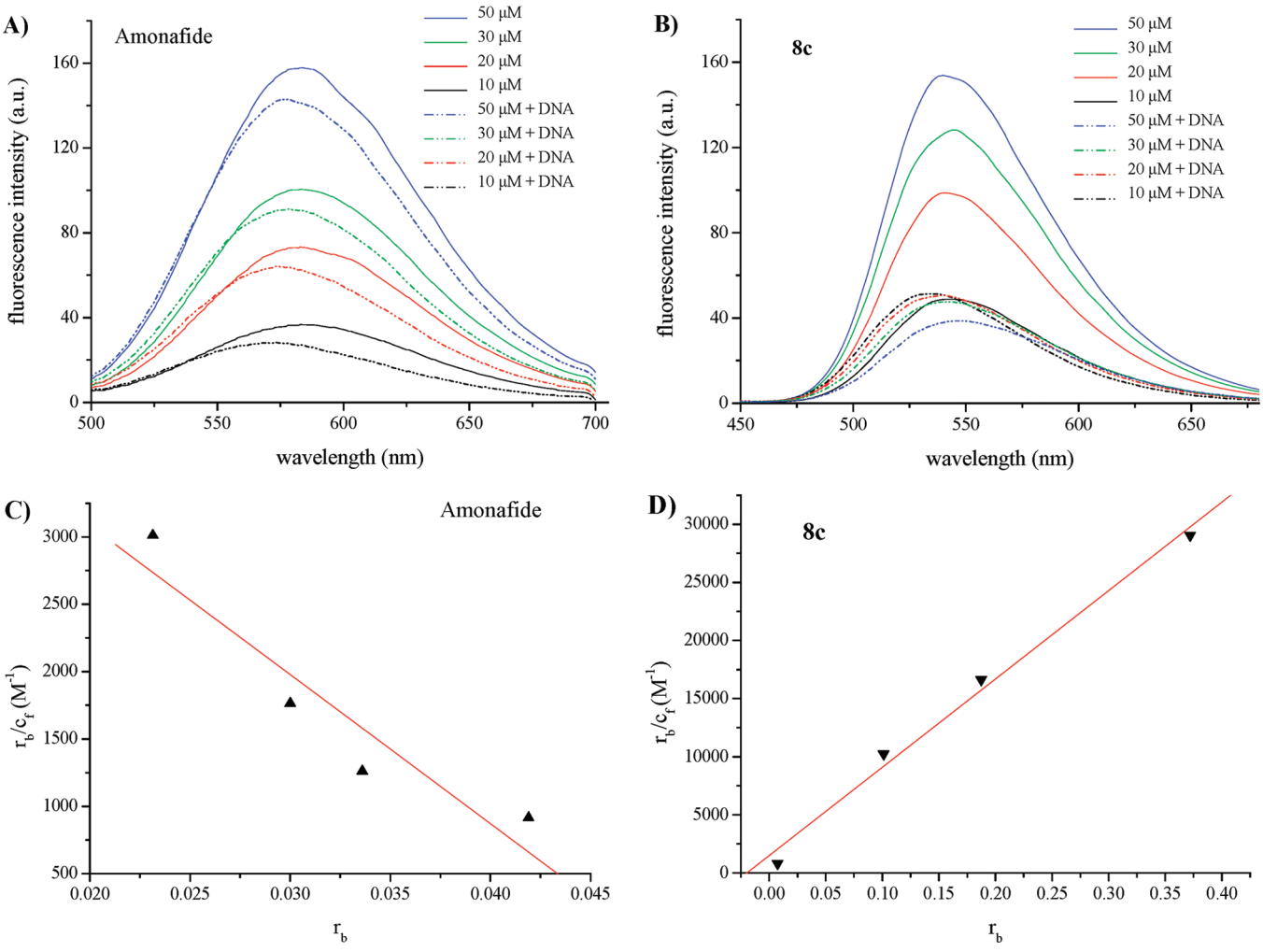

Figure 3. (A, B) Fluorescence spectra of amonafide and **8c** (10, 20, 30, 50 μM, respectively) before and after being incubated with CT DNA (100 μM). (C, D) Scatchard curve for amonafide and **8c** with CT DNA, respectively.

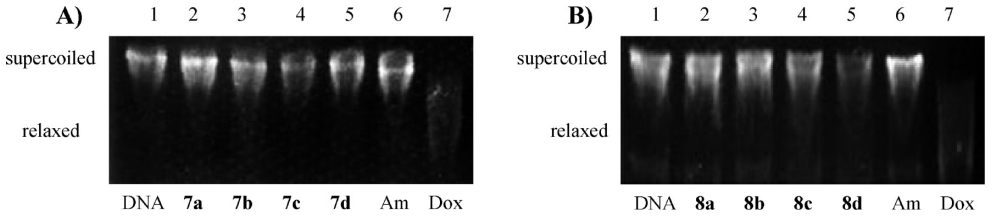

Figure 4. Gel electrophoresis of pBR322 DNA after being incubated with target compounds at the concentration of 100 μM for 2 h in Tris-HCl buffer (pH 7.4). (A) Lane 1, DNA alone; lanes 2−7, compounds **7a**−**d**, amonafide, and doxorubicin, respectively. (B) Lane 1, DNA alone; lanes 2−7, compounds **8a**−**d**, amonafide, and doxorubicin, respectively.

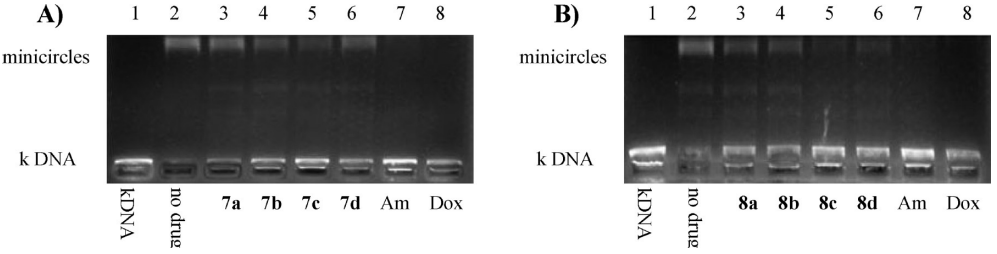

Figure 5. Inhibition of topo II-mediated kDNA decatenation by target compounds (100 μM). (A) Lane 1, kDNA; lane 2, minicircles (no drug); lanes 3−8, compounds **7a**−**d**, amonafide, and doxorubicin, respectively. (B) Lane 1, kDNA; lane 2, minicircles (no drug); lanes 3−8, compounds **8a**−**d**, amonafide, and doxorubicin, respectively.

most significant LMP was observed at the concentrations approximately equal to the IC_{50} values obtained in the antiproliferative cell-based assays, suggesting that LMP substantially contributed to the cytotoxicity of these compounds.

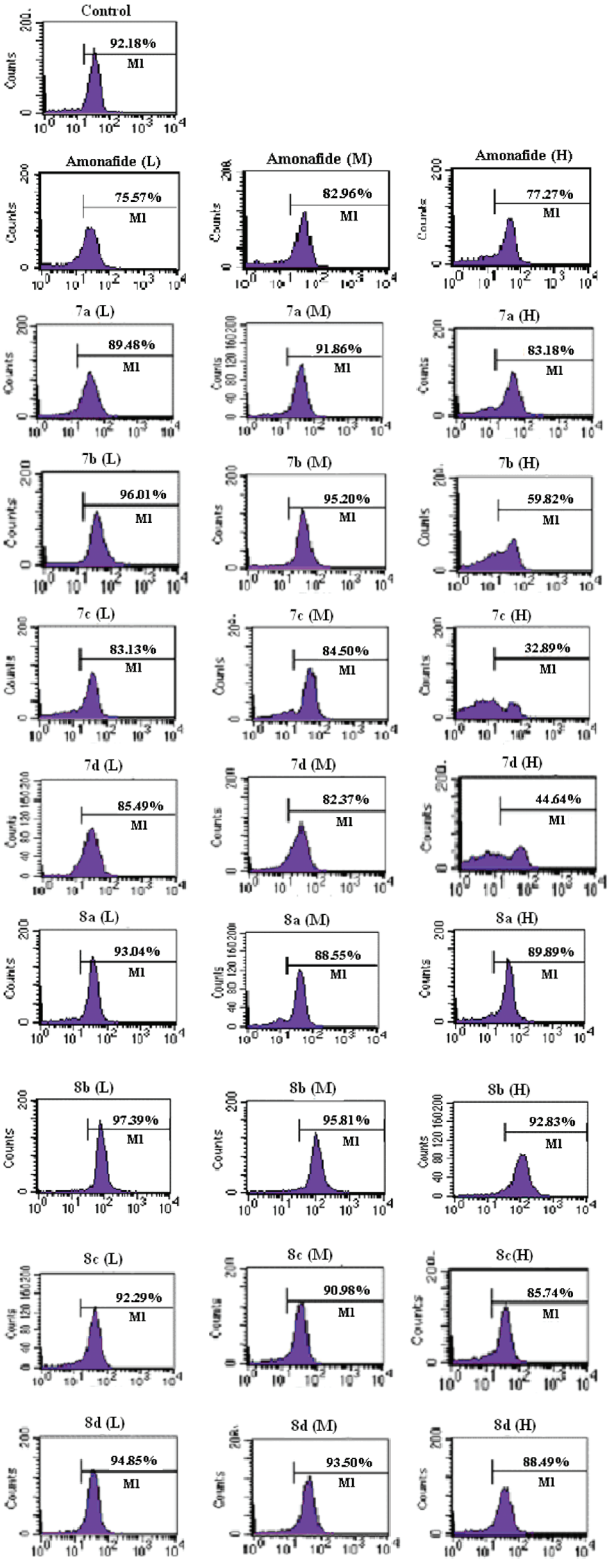

	drug concentration/μM		
	L	M	H
Am	5	10	15
7a	5	8	11
7b	1	3	5
7c	2	4	6
7d	2	4	6
8a	4	7	10
8b	2	4	6
8c	2	4	6
8d	14	17	20

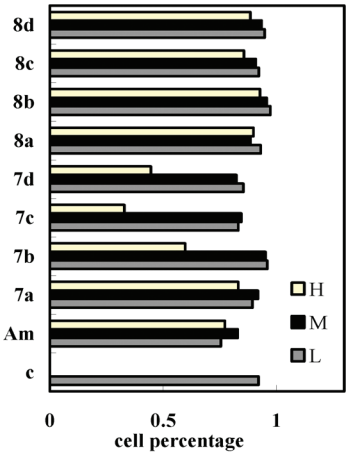

Figure 6. Drug-induced LMP. HeLa cells were stained with AO. Numbers indicate the percentage of cells with AO red fluorescence.

In contrast, analogues with the polyamine at the 6-position (**8a**−**d**) showed much weaker LMP induction than **7b**−**d**. The structure−activity relationships observed in the LMP experiments correlated well with the results obtained from the antiproliferative test. Additionally, no obvious LMP was observed at the test concentrations for amonafide, which indicated that the introduction of polyamine and long alkyl chain could provide the naphthalimide derivatives a novel target, LMP.

Induction of Cytochrome *c* Release. As demonstrated above, the new naphthalimides inhibited topo II, effectively induced LMP, and potently inhibit the growth of multiple cancer cell lines. Because either DNA damage or LMP could induce cell death through apoptosis, we investigated apoptosis as the cause of cell death. MOMP is considered to be one of the crucial checkpoints of apoptotic cell death[26,63] and could be detected by the release of cytochrome *c*.[61] Initiated

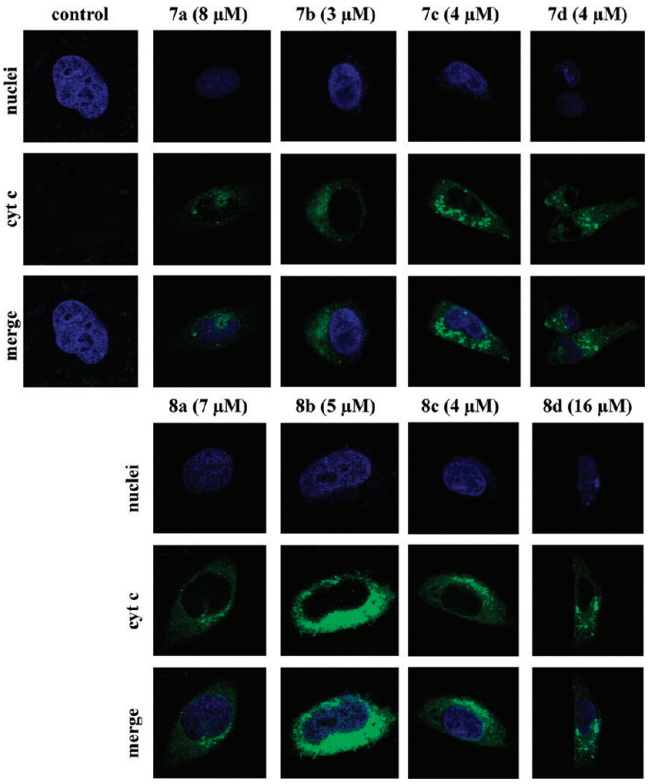

Figure 7. HeLa cells, untreated or treated with compounds **7a**−**d** and **8a**−**d**, were immunostained with rabbit anti-cytochrome *c* and FITC goat anti-rabbit IgG together with Hoechst 33258 nuclear staining.

by the loss of integrity of the outer mitochondrial membrane, cytochrome *c* and other intermembrane proteins are released into cytosol and then activate the downstream apoptotic machinery. Cytochrome *c* is a water-soluble protein, residing in the mitochondrial intermembrane spaces and serving as an electron shuttle in the respiratory chain in normal cells. Redistribution of cytochrome *c* into the cytosol is a crucial step in the mitochondrial-dependent apoptosis pathway, which leads to the formation of the apoptosome and then activates caspase 9 and caspase 3.[64] The cytochrome *c* distribution was *in situ* detected by double immunocytochemical staining in intact cells (see Figure 7).[65] Cells were labeled for cytochrome *c* (fluorescein isothiocyanate (FITC), green fluorescence) and nucleus (Hoechst 33258, blue fluorescence). As shown in Figure 7, the control cells without compound treatment exhibited no discernible immunofluorescence in the green emission channel. After being incubated with any of the target compounds **7a**−**d** and **8a**−**d** at the concentration corresponding the IC_{50} values, vivid green fluorescence was observed surrounding the nucleus of the HeLa cells, demonstrating that the new compounds induce significant cytochrome *c* release into cytosol from mitochondria and thereby confirming the MOMP-mediated apoptosis.

Apoptosis Assay by Annexin V Binding. To further illuminate drug-induced apoptosis, double staining for FITC-labeled annexin V binding to membrane phosphatidylserine (PS) and propidium iodide (PI) binding for cellular DNA was carried out and followed by flow cytometry. In the early stage of apoptosis, the membrane phospholipid PS is exported from the intracellular leaflet to the extracellular leaflet. The exposed PS binds to the phospholipid-binding protein annexin V in the presence of calcium, providing

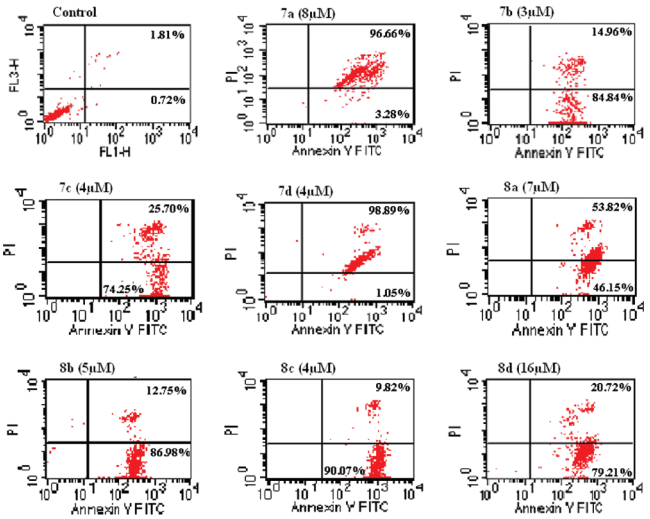

Figure 8. Apoptotic cells were detected with annexin V/PI double staining after incubation with compounds **7a**−**d** and **8a**−**d** for 24 h. The lower left quadrants represent live cells, the lower right quadrants are for early/primary apoptotic cells, upper right quadrants are for late/secondary apoptotic cells, while the upper left quadrants represent cells damaged during the procedure. The experiments were performed three times, and a representative experiment is shown.

a reliable method for quantifying the percentage of cells undergoing apoptosis using flow cytometry. The membrane-impermeable DNA-staining PI was used to detect cell membrane destruction in necrotic cells.[66,67] Different labeling patterns in this assay enable us to identify different cell populations: intact living cells (both annexin V and PI negative), early apoptotic cells (annexin V positive but PI negative), and late/secondary apoptotic cells (both annexin V and PI positive).[68,69] As shown in Figure 8, all tested compounds (**7a**−**d**, **8a**−**d**) at the concentration corresponding IC_{50} values very efficiently induced almost 100% apoptosis of HeLa cells. After incubation for 24 h, compounds **7b**, **c** and **8b**−**d** induced the major population of HeLa cells into the early apoptotic stage (84.84%, 74.25%, 86.98%, 90.07%, 79.21%, respectively), and compounds **7a** and **7d** induced the majority of the HeLa cells into the late apoptotic stage (96.66% and 98.89%, respectively). After incubation with compound **8a**, about half of the population of HeLa cells were in the early stage of apoptosis (46.15%) and the other half in the late stage (53.82%) of apoptosis.

Conclusion

We designed and synthesized a new class of naphthalimides with the structural features of the topo II inhibitor amonafide and lysosomotropic detergents. These new naphthalimides potently inhibited the growth of multiple cancer cell lines, and some of them were even more active than amonafide in the antiproliferative cell-based assays. The interactions of the new compounds with DNA were studied by CD spectra and fluorescence spectra, and the topo II inhibition activities were tested in a cell-free system, demonstrating that these compounds were weak DNA binders but inhibit topo II modestly. We further demonstrated that **7b**−**d** could also induce LMP, which was quite consistent with their favorable antiproliferative activity compared with their analogues, and thus preliminarily exhibited the advantages of multitarget drugs. To elucidate topo II and LMP-induced cell death pathways,

compounds **7a**−**d** and **8a**−**d** were tested and verified to efficiently induce apoptosis via a mitochondrial pathway as demonstrated by cytochrome *c* release and annexin V-FITC analysis. According to the encouraging results, a new design strategy could be deduced for the optimization of DNA intercalators for topo II inhibition. Further study of the antitumor mechanism of these novel multitarget drugs, especially cathepsin-related pathways, is still going on.

Experimental Section

All chemical reagents and solvents were purchased from commercial sources and used without further purification. Thin-layer chromatography (TLC) was performed on silica gel plates. Column chromatography was performed using silica gel (Hailang, Qingdao) 200−300 mesh. Melting points were determined using a Büchi melting point B-540 apparatus and are uncorrected. ^{1}H and ^{13}C NMR spectra were recorded employing a Bruker AV-400 spectrometer with chemical shifts expressed in parts per million (in deuteriochloroform, Me_4Si as internal standard). The mass spectra were collected at the Mass Instrumentation Facility of the Analysis and Research Center of ECUST. The purities of **7a**−**d**, **8a**−**d**, and **10a**−**d** were analyzed by HPLC, with the purity all being higher than 95%. Analytical HPLC was performed on a Hewlett-Packard 1100 system chromatograph equipped with photodiode array detector using a Zorbax Bonus-RP 5 μM 250 mm × 4.6 mm column (reverse phase) to detect the purity of the products. The mobile phase was a gradient of 70−100% methanol (solvent 1) and 10 mM NH_4OAc in water (pH 6.0) (solvent 2) at a flow rate of 1.0 mL/min (0−1.0 min, 70% solvent 1; 1.0−15.0 min, 70−100% solvent 1; 15.0−25.0 min, 100−70% solvent 1).

General Procedure for the Preparation of 1a, 2a,b, and 9a. To a stirred solution of 6-bromobenzo[*de*]isochromene-1,3-dione (1.94 g, 7.00 mmol) in EtOH (20 mL) was added the corresponding primary amine (7.70 mmol). The resulting mixture was heated at the refluxing temperature for 2−10 h and monitored by TLC. After completion, the reaction mixture was cooled to room temperature and concentrated under vacuum to give a solid, which was further purified.

6-Bromo-2-(3-hydroxypropyl)-1*H*-benzo[*de*]isoquinoline-1,3(2*H*)-dione (1a). The crude product was washed with water and then recrystallized from EtOH to give **1a**. White solid (yield 95%); mp 129.1−131.5 °C. ^{1}H NMR (400 MHz, $CDCl_3$): δ 8.68 (d, J = 7.2 Hz, 1H), 8.60 (d, J = 8.0 Hz, 1H), 8.43 (d, J = 7.6 Hz, 1H), 8.07 (d, J = 8 Hz, 1H), 7.87 (t, J = 8.0 Hz, 2H), 4.36 (t, J = 6.0 Hz, 2H), 3.62 (t, J = 6.0 Hz, 2H), 2.63 (br, 1H), 2.04−1.98 (m, 2H). MS (EI) calcd for $C_{15}H_{12}BrNO_3$ [M^+] 333.0, found 333.0.

6-Bromo-2-octyl-1*H*-benzo[*de*]isoquinoline-1,3(2*H*)-dione (2a). The crude product was washed with EtOH and then recrystallized from EtOH to give **2a**. White solid (yield 89%); mp 86.3−87.2 °C. ^{1}H NMR (400 MHz, $CDCl_3$): δ 8.68 (d, J = 7.2 Hz, 1H), 8.59 (d, J = 7.6 Hz, 1H), 8.44 (d, J = 8.0 Hz, 1H), 8.06 (d, J = 8.0 Hz, 1H), 7.87 (t, J = 7.6 Hz, 1H), 4.18 (t, J = 8.0 Hz, 2H), 1.78−1.71 (m, 2H), 1.47−1.29 (m, 10H), 0.89 (t, J = 7.2 Hz, 3H). MS (EI) calcd for $C_{20}H_{22}BrNO_2$ [M^+] 387.1, found 387.1.

6-Bromo-2-dodecyl-1*H*-benzo[*de*]isoquinoline-1,3(2*H*)-dione (2b). The crude product was first washed with EtOH and then recrystallized from EtOH to give **2b**. White solid (yield 85%); mp 66.6−67.4 °C. ^{1}H NMR (400 MHz, $CDCl_3$): δ 8.68 (d, J = 7.2 Hz, 1H), 8.59 (d, J = 8.4 Hz, 1H), 8.44 (d, J = 7.6 Hz, 1H), 8.06 (d, J = 8.0 Hz, 1H), 7.87 (t, J = 7.6 Hz, 1H), 4.18 (t, J = 7.6 Hz, 2H), 1.78−1.71 (m, 2H), 1.47−1.27 (m, 18H), 0.90 (t, J = 7.2 Hz, 3H). MS (EI) calcd for $C_{24}H_{30}BrNO_2$ [M^+] 443.1, found 443.2.

6-Bromo-2-(3-(dimethylamino)propyl)-1*H*-benzo[*de*]isoquinoline-1,3(2*H*)-dione (9a). The crude product was purified by column chromatography on silica gel (CH_2Cl_2/MeOH: 15/1) to provide **9a**. White solid (yield 92%); mp 99.4−100.8 °C. ^{1}H NMR (400 MHz, $CDCl_3$): δ 8.66 (d, J = 7.2 Hz, 1H), 8.57 (d, J = 8.8 Hz, 1H), 8.41 (d, J = 7.6 Hz, 1H), 8.04 (d, J = 8.0 Hz, 1H), 7.85 (t, J = 8.0 Hz, 1H), 4.23 (t, J = 7.6 Hz, 2H), 2.45 (t, J = 7.2 Hz, 2H), 2.27 (s, 6H), 1.96−1.89 (m, 2H). MS (EI) calcd for $C_{17}H_{17}BrN_2O_2$ [M^+] 360.0, found 360.1.

General Procedure for the Preparation of 3a,b, 4a,b, and 10a,b,d. To a stirred solution of the amination intermediate (5.00 mmol) in 2-methoxyethanol (15 mL) was added the corresponding primary amine (15.00 mmol). The mixture was then heated at the refluxing temperature for 6−12 h and monitored by TLC. After completion, the reaction mixture was cooled to room temperature and concentrated under vacuum until most of the solvent was removed. The residue was further purified.

2-(3-Hydroxypropyl)-6-(octylamino)-1*H*-benzo[*de*]isoquinoline-1,3(2*H*)-dione (3a). The residue was washed with EtOH and then purified by column chromatography on silica gel (CH_2Cl_2/MeOH: 18/1) to provide **3a**. Yellow solid (yield 90%); mp 146.7−149.4 °C. ^{1}H NMR (400 MHz, $CDCl_3$): δ 8.62 (d, J = 8.0 Hz, 1H), 8.50 (d, J = 8.4 Hz, 1H), 8.13 (d, J = 8.0 Hz, 1H), 7.65 (t, J = 8.0 Hz, 1H), 6.75 (d, J = 8.4 Hz, 1H), 4.36 (t, J = 6.0 Hz, 2H), 3.57 (t, J = 5.6 Hz, 2H), 3.43 (t, J = 7.2 Hz, 2H), 2.02−1.97 (m, 2H), 1.87−1.80 (m, 2H), 1.56−1.32 (m, 10H), 0.91 (t, J = 6.8 Hz, 3H). MS (ESI) calcd for $C_{23}H_{31}N_2O_3$ [$M + H]^+$ 383.2, found 383.2.

6-(Dodecylamino)-2-(3-hydroxypropyl)-1*H*-benzo[*de*]isoquinoline-1,3(2*H*)-dione (3b). The residue was washed with EtOH and then purified by column chromatography on silica gel (CH_2Cl_2/MeOH: 18/1) to provide **3b**. Yellow solid (yield 83%); mp 144.9−146.4 °C. ^{1}H NMR (400 MHz, $CDCl_3$): δ 8.62 (d, J = 6.4 Hz, 1H), 8.50 (d, J = 8.4 Hz, 1H), 8.13 (d, J = 8.4 Hz, 1H), 7.66 (t, J = 8.0 Hz, 1H), 6.76 (d, J = 8.4 Hz, 1H), 4.36 (t, J = 6.0 Hz, 2H), 3.57 (t, J = 5.6 Hz, 2H), 3.44 (t, J = 7.2 Hz, 2H), 2.03−1.97 (m, 2H), 1.87−1.80 (m, 2H), 1.56−1.29 (m, 18H), 0.90 (t, J = 6.4 Hz, 3H). MS (ESI) calcd for $C_{27}H_{38}N_2O_3Na$ [$M + Na]^+$ 461.3, found 461.3.

6-(2-Hydroxyethylamino)-2-octyl-1*H*-benzo[*de*]isoquinoline-1,3(2*H*)-dione (4a). The residue was washed with water and then purified by column chromatography on silica gel (CH_2Cl_2/MeOH: 20/1) to provide **4a**. Yellow solid (yield 85%); mp 156.0−157.8 °C. ^{1}H NMR (400 MHz, $CDCl_3$): δ 8.57 (d, J = 7.2 Hz, 1H), 8.45 (d, J = 8.4 Hz, 1H), 8.13 (d, J = 8.4 Hz, 1H), 7.62 (t, J = 7.6 Hz, 1H), 6.74 (d, J = 8.4 Hz, 1H), 4.16 (t, J = 8.0 Hz, 2H), 4.09 (t, J = 5.2 Hz, 2H), 3.60 (t, J = 5.2 Hz, 2H), 1.77−1.70 (m, 2H), 1.47−1.28 (m, 10H), 0.89 (t, J = 7.2 Hz, 3H). MS (ESI) calcd for $C_{22}H_{29}N_2O_3$ [$M + H]^+$ 369.2, found 369.2.

2-Dodecyl-6-(2-hydroxyethylamino)-1*H*-benzo[*de*]isoquinoline-1,3(2*H*)-dione (4b). The residue was washed with water and then purified by column chromatography on silica gel (CH_2Cl_2/MeOH: 20/1) to provide **4b**. Yellow solid (yield 85%); mp 149.9−152.2 °C. ^{1}H NMR (400 MHz, $CDCl_3$): δ 8.53 (d, J = 7.2 Hz, 1H), 8.41(d, J = 8.4 Hz, 1H), 8.11 (d, J = 8.0 Hz, 1H), 7.59 (t, J = 8.0 Hz, 1H), 6.71 (d, J = 8.4 Hz, 1H), 4.15 (t, J = 7.6 Hz, 2H), 4.09 (t, J = 5.2 Hz, 2H), 3.58 (t, J = 5.2 Hz, 2H), 1.76−1.69 (m, 2H), 1.45−1.26 (m, 18H), 0.89 (t, J = 7.2 Hz, 3H). MS (ESI) calcd for $C_{26}H_{37}N_2O_3$ [$M + H]^+$ 425.3, found 425.3.

2-Dodecyl-6-(octylamino)-1*H*-benzo[*de*]isoquinoline-1,3(2*H*)-dione (10a). The residue was washed with EtOH and then purified by column chromatography on silica gel (petroleum ether/CH_2Cl_2: 1/2) to provide **10a**. Yellow solid (yield 89%); mp 92.8−94.1 °C. ^{1}H NMR (400 MHz, $CDCl_3$): δ 8.56 (d, J = 7.2 Hz, 1H), 8.44 (d, J = 8.4 Hz, 1H), 8.11 (d, J = 8.0 Hz, 1H), 7.58 (t, J = 8.0 Hz, 1H), 6.70 (d, J = 8.4 Hz, 1H), 5.41 (br, 1H), 4.16 (t, J = 7.6 Hz, 2H), 3.39 (t, J = 7.2 Hz, 2H), 1.85−1.69 (m, 4H), 1.53−1.25 (m, 28H), 0.91−0.87 (m, 6H). ^{13}C NMR (100 MHz, $CDCl_3$): δ 164.66, 164.12, 149.46, 134.42, 131.01, 129.78, 125.81, 124.57, 123.16, 120.16, 110.18, 104.26, 43.76, 40.24, 31.93, 31.79, 29.63, 29.60, 29.45, 29.35, 29.22, 28.99, 28.25, 27.23, 27.20, 22.69, 22.64, 14.13, 14.09. HRMS (ESI) calcd for $C_{32}H_{49}N_2O_2$ [$M + H]^+$ 493.3794, found 493.3780.

6-(2-(Dimethylamino)ethylamino)-2-dodecyl-1*H*-benzo[*de*]isoquinoline-1,3(2*H*)-dione (10b). The residue was poured onto water (100 mL) and then extracted with $CHCl_3$ (3 × 100 mL). The combined organic layers were dried over $MgSO_4$ and concentrated. The crude product was purified by column chromatography on silica gel (CH_2Cl_2/MeOH: 25/1) to provide **10b**. Orange solid (yield 82%); mp 97.6−99.2 °C. ^{1}H NMR (400 MHz, $CDCl_3$): δ 8.55 (d, J = 7.2 Hz, 1H), 8.42 (d, J = 8.4 Hz, 1H), 8.11 (d, J = 8.0 Hz, 1H), 7.59 (t, J = 8.0 Hz, 1H), 6.63 (d, J = 8.4 Hz, 1H), 6.28 (t, J = 3.6 Hz, 1H), 4.14 (t, J = 7.6 Hz, 2H), 3.38−3.34 (m, 2H), 2.72 (t, J = 5.6 Hz, 2H), 2.33 (s, 6H), 1.75−1.68 (m, 2H), 1.45−1.24 (m, 18H), 0.87 (t, J = 6.4 Hz, 3H). ^{13}C NMR (100 MHz, $CDCl_3$): δ 164.62, 164.05, 149.54, 134.39, 130.93, 129.65, 126.30, 124.47, 122.92, 120.26, 109.98, 104.27, 56.87, 45.04, 40.17, 40.12, 31.91, 29.62, 29.44, 29.34, 28.23, 27.23, 22.68, 14.13. HRMS (ESI) calcd for $C_{28}H_{42}N_3O_2$ $[M + H]^+$ 452.3277, found 452.3254.

2-(3-(Dimethylamino)propyl)-6-(octylamino)-1*H*-benzo[*de*]isoquinoline-1,3(2*H*)-dione (10d). The residue was poured onto water (100 mL) and then extracted with $CHCl_3$ (3 × 100 mL). The combined organic layers were dried over $MgSO_4$ and concentrated. The crude product was purified by column chromatography on silica gel (CH_2Cl_2/MeOH: 25/1) to provide **10d**. Orange solid (yield 83%); mp 56.3−59.8 °C. ^{1}H NMR (400 MHz, $CDCl_3$): δ 8.33−8.29 (m, 1H), 8.24−8.20 (m, 2H), 7.37−7.32 (m, 1H), 6.49−6.45 (m, 1H), 6.16 (br, 1H), 4.06 (t, J = 7.2 Hz, 2H), 3.27−3.22 (m, 2H), 2.28 (t, J = 7.2 Hz, 2H), 2.10 (s, 6H), 1.82−1.74 (m, 2H), 1.69−1.61 (m, 2H), 1.33−1.10 (m, 10H), 0.75−0.70 (m, 3H). ^{13}C NMR (100 MHz, $CDCl_3$): δ 164.53, 163.91, 150.04, 134.33, 130.76, 129.66, 126.90, 124.17, 122.46, 120.16, 109.07, 103.86, 57.27, 45.30, 43.63, 38.32, 31.68, 29.28, 29.14, 28.71, 27.16, 26.18, 22.52, 14.01. HRMS (ESI) calcd for $C_{25}H_{36}N_3O_2$ $[M + H]^+$ 410.2808, found 410.2798.

2-(3-(Dimethylamino)propyl)-6-(methylamino)-1*H*-benzo[*de*]isoquinoline-1,3(2*H*)-dione (10c). Compound **9a** (502 mg, 1.39 mmol) and $CuSO_4 \cdot 5H_2O$ (872 mg, 3.48 mmol) were added to 40% methylamine aqueous solution (20 mL). The mixture was then heated at the refluxing temperature for 4 h and monitored by TLC. After completion, the reaction mixture was cooled to room temperature and concentrated under vacuum. The resulting mixture was diluted with water (30 mL) containing 10% NaCl and 1% Na_2CO_3 and extracted with CH_2Cl_2 (3 × 50 mL). The organic layer was then concentrated under vacuum and then further purified by column chromatography on silica gel (CH_2Cl_2/MeOH: 10/1) to provide **10c**. Orange solid (yield 86%); mp 169.9−170.6 °C. ^{1}H NMR (400 MHz, $CDCl_3$): δ 8.48 (d, J = 7.2 Hz, 1H), 8.40 (d, J = 8.4 Hz, 1H), 8.09 (d, J = 8.4 Hz, 1H), 7.52 (t, J = 8.0 Hz, 1H), 6.62 (d, J = 8.8 Hz, 1H), 5.75 (br, 1H), 4.19 (t, J = 7.6 Hz, 2H), 3.10 (d, J = 4.8 Hz, 3H), 2.44 (t, J = 7.6 Hz, 2H), 2.26 (s, 6H), 1.95−1.87 (m, 2H). ^{13}C NMR (100 MHz, $CDCl_3$): δ 164.63, 164.11, 150.44, 134.41, 130.94, 129.61, 126.03, 124.56, 122.93, 120.22, 110.09, 103.82, 57.35, 45.35, 38.44, 30.44, 26.17. HRMS (ESI) calcd for $C_{18}H_{22}N_3O_2$ $[M + H]^+$ 312.1712, found 312.1721.

General Procedure for the Preparation of 5a,b and 6a,b. To a stirred solution of DDQ (409 mg, 1.80 mmol) and PPh_3 (472 mg, 1.80 mmol) in dry CH_2Cl_2 was added (n-butyl)$_4$NBr (580 mg, 1.80 mmol) at room temperature. **3a**,**b** or **4a**,**b** (1.50 mmol) was then added to this mixture, which immediately turned the yellow color of the reaction mixture to deep red. The mixture was stirred at room temperature for 24 h. The solvent was then removed under vacuum to fifth of the volume. The residue was purified by column chromatography on silica gel using pure CH_2Cl_2 as eluant to give the corresponding bromide product.

2-(3-Bromopropyl)-6-(octylamino)-1*H*-benzo[*de*]isoquinoline-1,3(2*H*)-dione (5a). Orange solid (yield 75%); mp 93.4−94.8 °C. ^{1}H NMR (400 MHz, $CDCl_3$): δ 8.60 (d, J = 7.2 Hz, 1H), 8.48 (d, J = 8.8 Hz, 1H), 8.11 (d, J = 8.4 Hz, 1H), 7.64 (t, J = 8.0 Hz, 1H), 6.74 (d, J = 8.4 Hz, 1H), 5.32 (br, 1H), 4.32 (t, J = 7.2 Hz, 2H), 3.51 (t, J = 7.2 Hz, 2H), 3.42 (t, J = 7.2 Hz, 2H), 2.38−2.31 (m, 2H), 1.87−1.80 (m, 2H), 1.55−1.32 (m, 10H), 0.91 (t, J = 6.8 Hz, 3H). MS (ESI) calcd for $C_{23}H_{30}BrN_2O_2$ $[M + H]^+$ 445.1, found 445.2.

2-(3-Bromopropyl)-6-(dodecylamino)-1*H*-benzo[*de*]isoquinoline-1,3(2*H*)-dione (5b). Orange solid (yield 72%); mp 54.9−57.3 °C. ^{1}H NMR (400 MHz, $CDCl_3$): δ 8.60 (d, J = 7.6 Hz, 1H), 8.48 (d, J = 8.4 Hz, 1H), 8.11 (d, J = 8.0 Hz, 1H), 7.64 (t, J = 8.0 Hz, 1H), 6.75 (d, J = 8.4 Hz, 1H), 5.30 (br, 1H), 4.32 (t, J = 6.8 Hz, 2H), 3.51 (t, J = 7.2 Hz, 2H), 3.43 (t, J = 7.2 Hz, 2H), 2.38−2.31 (m, 2H), 1.87−1.80 (m, 2H), 1.55−1.29 (m, 18H), 0.90 (t, J = 6.8 Hz, 3H). MS (ESI) calcd for $C_{27}H_{37}N_2O_2$ $[M - Br]^+$ 421.3, found 421.3.

6-(2-Bromoethylamino)-2-octyl-1*H*-benzo[*de*]isoquinoline-1,3(2*H*)-dione (6a). Orange solid (yield 82%); mp 146.2−147.3 °C. ^{1}H NMR (400 MHz, $CDCl_3$): δ 8.63 (d, J = 6.4 Hz, 1H), 8.50 (d, J = 8.4 Hz, 1H), 8.16 (d, J = 7.6 Hz, 1H), 7.69 (t, J = 8.0 Hz, 1H), 6.77 (d, J = 8.4 Hz, 1H), 5.60 (br, 1H), 4.17 (t, J = 7.6 Hz, 2H), 3.89 (q, J = 4.4 Hz, 2H), 3.77 (t, J = 6.0 Hz, 2H), 1.78−1.70 (m, 2H), 1.47−1.28 (m, 10H), 0.89 (t, J = 7.2 Hz, 3H). MS (ESI) calcd for $C_{22}H_{28}BrN_2O_2$ $[M + H]^+$ 431.1, found 431.2.

6-(2-Bromoethylamino)-2-dodecyl-1*H*-benzo[*de*]isoquinoline-1,3(2*H*)-dione (6b). Orange solid (yield 80%); mp 123.9−126.0 °C. ^{1}H NMR (400 MHz, $CDCl_3$): δ 8.63 (d, J = 7.2 Hz, 1H), 8.50 (d, J = 8.4 Hz, 1H), 8.16 (d, J = 8.0 Hz, 1H), 7.69 (t, J = 8.4 Hz, 1H), 6.77 (d, J = 8.4 Hz, 1H), 5.60 (br, 1H), 4.17 (t, J = 7.6 Hz, 2H), 3.89 (t, J = 5.6 Hz, 2H), 3.77 (t, J = 6.0 Hz, 2H), 1.78−1.70 (m, 2H), 1.45−1.27 (m, 18H), 0.90 (t, J = 7.2 Hz, 3H). MS (ESI) calcd for $C_{26}H_{36}$ BrN_2O_2 $[M + H]^+$ 487.2, found 487.2.

General Procedure for the Preparation of 7a−d and 8a−d. To a stirred solution of the bromide precursor (0.225 mmol) and KI (45 mg, 0.271 mmol) in dry $CHCl_3$ was added the corresponding polyamine (1.12 mmol) under argon. The mixture was heated at the refluxing temperature for 48 h. The reaction mixture was then cooled to room temperature and concentrated under vacuum. The resulting mixture was diluted with water (10 mL) containing 10% NaCl and 1% Na_2CO_3 and extracted with CH_2Cl_2 (3 × 15 mL). The organic layer was then concentrated under vacuum and then further purified.

2-(3-(4-Methylpiperazin-1-yl)propyl)-6-(octylamino)-1*H*-benzo[*de*]isoquinoline-1,3(2*H*)-dione (7a). The crude product was purified by column chromatography on silica gel (CH_2Cl_2/MeOH/Et_3N: 100/4/1) to provide **7a**. Orange amorphous solid (yield 72%). ^{1}H NMR (400 MHz, $CDCl_3$): δ 8.51 (d, J = 7.6 Hz, 1H), 8.40 (d, J = 8.4 Hz, 1H), 8.10 (d, J = 7.6 Hz, 1H), 7.54 (t, J = 7.6 Hz, 1H), 6.66 (d, J = 8.4 Hz, 1H), 5.45 (br, 1H), 4.19 (t, J = 7.2 Hz, 2H), 3.39−3.34 (m, 2H), 2.81−2.37 (m, 10H), 2.21 (s, 3H), 1.95−1.88 (m, 2H), 1.82−1.75 (m, 2H), 1.50−1.24 (m, 10H), 0.87 (t, J = 6.4 Hz, 3H). ^{13}C NMR (100 MHz, $CDCl_3$): δ 164.68, 164.12, 149.53, 134.42, 130.98, 129.79, 125.89, 124.54, 123.08, 120.15, 110.04, 104.23, 56.09, 55.08, 52.97, 45.96, 43.74, 38.57, 31.76, 29.32, 29.19, 28.95, 27.17, 25.28, 22.61, 14.07. HRMS (ESI) calcd for $C_{28}H_{41}N_4O_2$ $[M + H]^+$ 465.3230, found 465.3209.

6-(Dodecylamino)-2-(3-(4-methylpiperazin-1-yl)propyl)-1*H*-benzo[*de*]isoquinoline-1,3(2*H*)-dione (7b). The crude product was purified by column chromatography on silica gel (CH_2Cl_2/MeOH/Et_3N: 100/4/1) to provide **7b**. Orange amorphous solid (yield 70%). ^{1}H NMR (400 MHz, $CDCl_3$): δ 8.52 (d, J = 7.2 Hz, 1H), 8.41 (d, J = 8.4 Hz, 1H), 8.10 (d, J = 7.6 Hz, 1H), 7.55 (t, J = 8.0 Hz, 1H), 6.67 (d, J = 8.4 Hz, 1H), 5.43 (br, 1H), 4.20 (t, J = 7.6 Hz, 2H), 3.40−3.35 (m, 2H), 2.81−2.38 (m, 10H), 2.21 (s, 3H), 1.95−1.88 (m, 2H), 1.83−1.75 (m, 2H), 1.51−1.25 (m, 18H), 0.87 (t, J = 6.4 Hz, 3H). ^{13}C NMR (100 MHz, $CDCl_3$): δ 164.67, 164.11, 149.51, 134.41, 130.97, 129.78, 125.86, 124.53, 123.09, 120.14, 110.06, 104.23, 56.09, 55.09, 52.98, 45.97, 43.74, 38.57, 31.88, 29.60, 29.54, 29.36, 29.31, 28.96, 27.17, 25.28, 22.66, 14.10. HRMS (ESI) calcd for $C_{32}H_{49}N_4O_2$ $[M + H]^+$ 521.3856, found 521.3862.

2-(3-(2-(Dimethylamino)ethylamino)propyl)-6-(octylamino)-1*H*-benzo[*de*]isoquinoline-1,3(2*H*)-dione (7c). The crude product was purified by column chromatography on silica gel (CH_2Cl_2/MeOH/Et_3N: 100/5/1) to provide **7c**. Orange amorphous solid

(yield 65%). ^{1}H NMR (400 MHz,$CDCl_3$): δ 8.48 (d, J = 7.2 Hz, 1H), 8.37 (d, J = 8.4 Hz, 1H), 8.11 (d, J = 8.4 Hz, 1H), 7.52 (t, J = 8.0 Hz, 1H), 6.63 (d, J = 8.8 Hz, 1H), 5.59 (br, 1H), 4.20 (t, J = 6.8 Hz, 2H), 3.37−3.33 (m, 2H), 2.70−2.64 (m, 4H), 2.37 (t, J = 6.0 Hz, 2H), 2.17 (s, 6H), 1.96−1.89 (m, 2H), 1.80−1.73 (m, 2H), 1.48−1.22 (m, 10H), 0.85 (t, J = 6.8 Hz, 3H). ^{13}C NMR (100 MHz, $CDCl_3$): δ 164.69, 164.11, 149.65, 134.48, 131.02, 129.75, 126.10, 124.48, 122.87, 120.12, 109.74, 104.17, 59.23, 47.45, 47.30, 45.57, 43.71, 38.00, 31.76, 29.33, 29.20, 28.90, 28.51, 27.18, 22.62, 14.09. HRMS (ESI) calcd for $C_{27}H_{41}N_4O_2$ $[M + H]^+$ 453.3230, found 453.3222.

2-(3-(2-(Dimethylamino)ethylamino)propyl)-6-(dodecylamino)-1*H*-benzo[*de*]isoquinoline-1,3(2*H*)-dione (7d). The crude product was purified by column chromatography on silica gel (CH_2Cl_2/MeOH/Et_3N: 100/5/1) to provide **7d**. Orange amorphous solid (yield 60%). ^{1}H NMR (400 MHz, $CDCl_3$): δ 8.49 (d, J = 7.2 Hz, 1H), 8.39 (d, J = 8.4 Hz, 1H), 8.11 (d, J = 8.4 Hz, 1H), 7.53 (t, J = 8.0 Hz, 1H), 6.65 (d, J = 8.4 Hz, 1H), 5.54 (br, 1H), 4.21 (t, J = 6.8 Hz, 2H), 3.38−3.33 (m, 2H), 2.70−2.64 (m, 4H), 2.37 (t, J = 6.0 Hz, 2H), 2.18 (s, 6H), 1.96−1.89 (m, 2H), 1.81−1.74 (m, 2H), 1.45−1.23 (m, 18H), 0.85 (t, J = 7.2 Hz, 3H). ^{13}C NMR (100 MHz, $CDCl_3$): δ 164.68, 164.11, 149.61, 134.47, 131.01, 129.76, 126.03, 124.49, 122.92, 120.13, 109.82, 104.18, 59.28, 47.48, 47.32, 45.58, 43.71, 38.02, 31.88, 29.60, 29.57, 29.37, 29.32, 28.91, 28.54, 27.18, 22.66, 14.12. HRMS (ESI) calcd for $C_{31}H_{49}N_4O_2$ $[M + H]^+$ 509.3856, found 509.3848.

6-(2-(4-Methylpiperazin-1-yl)ethylamino)-2-octyl-1*H*-benzo[*de*]isoquinoline-1,3(2*H*)-dione (8a). The crude product was purified by column chromatography on silica gel (CH_2Cl_2/MeOH/Et_3N: 100/4/1) to provide **8a**. Orange solid (yield 85%); mp 109.6−113.6 °C. ^{1}H NMR (400 MHz, $CDCl_3$): δ 8.49−8.46 (m, 1H), 8.37−8.33 (m, 1H), 8.19 (d, J = 8.4 Hz, 1H), 7.59−7.53 (m, 1H), 6.59−6.57 (m, 1H), 6.34 (br, 1H), 4.11−4.06 (m, 2H), 3.47−3.43 (m, 2H), 2.92−2.87 (m, 10H), 2.56 (s, 3H), 1.71−1.63 (m, 2H), 1.36−1.22 (m, 10H), 0.83 (t, J = 6.4 Hz, 3H). ^{13}C NMR (100 MHz, $CDCl_3$): δ 164.53, 163.98, 149.25, 134.23, 130.97, 129.60, 126.54, 124.72, 122.89, 120.36, 110.32, 104.29, 55.23, 54.22, 51.02, 44.74, 40.19, 39.32, 31.80, 29.66, 29.37, 29.22, 28.21, 27.21, 22.61, 14.08. HRMS (ESI) calcd for $C_{27}H_{39}N_4O_2$ $[M + H]^+$ 451.3073, found 451.3085.

2-Dodecyl-6-(2-(4-methylpiperazin-1-yl)ethylamino)-1*H*-benzo[*de*]isoquinoline-1,3(2*H*)-dione (8b). The crude product was purified by column chromatography on silica gel (CH_2Cl_2/MeOH/Et_3N: 100/4/1) to provide **8b**. Orange amorphous solid (yield 81%). ^{1}H NMR (400 MHz, $CDCl_3$): δ 8.50−8.46 (m, 1H), 8.36−8.32 (m, 1H), 8.23 (d, J = 8.4 Hz, 1H), 7.58−7.53 (m, 1H), 6.60−6.57 (m, 1H), 6.39 (br, 1H), 4.10−4.06 (m, 2H), 3.49−3.45 (m, 2H), 2.95−2.92 (m, 10H), 2.59 (s, 3H), 1.70−1.62 (m, 2H), 1.36−1.20 (m, 18H), 0.84 (t, J = 6.8 Hz, 3H). ^{13}C NMR (100 MHz, $CDCl_3$): δ 164.51, 163.96, 149.21, 134.20, 130.98, 129.59, 126.63, 124.72, 122.88, 120.39, 110.40, 104.24, 55.21, 53.95, 50.76, 44.50, 40.19, 39.32, 31.87, 29.66, 29.59, 29.42, 29.31, 28.21, 27.21, 22.65, 14.10. HRMS (ESI) calcd for $C_{31}H_{47}N_4O_2$ $[M + H]^+$ 507.3699, found 507.3686.

6-(2-(2-(Dimethylamino)ethylamino)ethylamino)-2-octyl-1*H*-benzo[*de*]isoquinoline-1,3(2*H*)-dione (8c). The crude product was purified by column chromatography on silica gel (CH_2Cl_2/MeOH/Et_3N: 100/5/1) to provide **8c**. Orange amorphous solid (yield 79%). ^{1}H NMR (400 MHz, $CDCl_3$): δ 8.51 (d, J = 7.2 Hz, 1H), 8.39 (d, J = 8.0 Hz, 1H), 8.14 (d, J = 8.4 Hz, 1H), 7.54 (t, J = 8.0 Hz, 1H), 6.61 (d, J = 8.4 Hz, 1H), 6.42 (br, 1H), 4.12 (t, J = 7.6 Hz, 2H), 3.41−3.37 (m, 2H), 3.07 (t, J = 5.2 Hz, 2H), 2.75 (t, J = 5.6 Hz, 2H), 2.44 (t, J = 5.6 Hz, 2H), 2.23 (s, 6H), 1.74−1.66 (m, 2H), 1.41−1.24 (m, 10H), 0.85 (t, J = 6.8 Hz, 3H). ^{13}C NMR (100 MHz, $CDCl_3$): δ 164.69, 164.13, 149.76, 134.46, 130.96, 129.72, 126.47, 124.43, 122.92, 120.38, 109.93, 104.28, 58.86, 47.28, 46.38, 45.50, 42.22, 40.20, 31.84, 29.41, 29.26, 28.23, 27.23, 22.65, 14.12. HRMS (ESI) calcd for $C_{26}H_{39}N_4O_2$ $[M + H]^+$ 439.3073, found 439.3075.

6-(2-(2-(Dimethylamino)ethylamino)ethylamino)-2-dodecyl-1*H*-benzo[*de*]isoquinoline-1,3(2*H*)-dione (8d). The crude product was purified by column chromatography on silica gel (CH_2Cl_2/MeOH/Et_3N: 100/5/1) to provide **8d**. Orange solid (yield 73%); mp 68.4−69.6 °C. ^{1}H NMR (400 MHz, $CDCl_3$): δ 8.54 (d, J = 7.2 Hz, 1H), 8.42 (d, J = 8.4 Hz, 1H), 8.17 (d, J = 8.4 Hz, 1H), 7.57 (t, J = 8.0 Hz, 1H), 6.64 (d, J = 8.4 Hz, 1H), 6.42 (br, 1H), 4.14 (t, J = 7.6 Hz, 2H), 3.43−3.39 (m, 2H), 3.09 (t, J = 5.2 Hz, 2H), 2.77 (t, J = 6.0 Hz, 2H), 2.46 (t, J = 5.6 Hz, 2H), 2.25 (s, 6H), 1.75−1.68 (m, 2H), 1.43−1.24 (m, 18H), 0.87 (t, J = 6.4 Hz, 3H). ^{13}C NMR (100 MHz, $CDCl_3$): δ 164.71, 164.15, 149.76, 134.47, 130.99, 129.76, 126.48, 124.48, 122.98, 120.43, 110.03, 104.29, 58.83, 47.28, 46.35, 45.47, 42.23, 40.21, 31.92, 29.63, 29.60, 29.46, 29.36, 28.24, 27.24, 22.69, 14.14. HRMS (ESI) calcd for $C_{30}H_{47}N_4O_2$ $[M + H]^+$ 495.3699, found 495.3699.

***In Vitro* Cytotoxicity Assays.** MTT assays were utilized to assess the *in vitro* antiproliferative potencies of the target compounds against HeLa, HL-60, MCF-7, MKN45, and LS174 cells. All cells were purchased from Cell Bank of Type Culture Collection of Chinese Academy of Sciences (Shanghai, China). MTT is a water-soluble tetrazolium salt, which can be transformed into colored, water-insoluble formazan crystals by mitochondrial dehydrogenases in living cells. Ten thousand cells were plated in 96-well dishes and incubated for 24 h. The tested compounds in dimethyl sulfoxide (DMSO) solution were added ranging from 0 to 25 μM. After 24 h treatment, cell viability was evaluated by MTT assay. Briefly, cells were incubated with MTT solution (500 μg/mL) for 4 h at 37 °C, and then 100 μL per well of DMSO was added to replace MTT-containing medium and to dissolve the reaction product formazan salts by gentle shaking for 10 min. The absorbance at 570 nm in control and drug-treated wells was measured using an automated microplate reader (Multiskan Ex; Lab systems, Finland). The IC_{50}, which represents the drug concentration required for 50% growth inhibition of cells, was extracted from linear regression analysis of experimental data to express cytotoxicity. Each experiment was repeated in triplicate.

DNA Intercalating Assay by CD Spectra. CT DNA was purchased from Sigma Aldrich and used without further purification. A solution of CT DNA in 20 mM Tris-HCl buffer (pH 7.4) was stored at 4 °C and used after no more than 4 days. The concentration of CT DNA was determined spectrophotometrically from the molar absorption coefficient (6600 M^{-1} cm^{-1}). The stock solution was attested to be sufficiently free from protein, as it gave a UV absorbance ratio at 260 and 280 nm of more than 1.8.

The CD measurements were performed on a J-815 spectrophotometer (Jasco, Japan) using 1 cm quartz cell in the range of 200−400 nm. The samples containing 100 μM CT DNA and 20 μM drugs in Tris-HCl buffer were recorded of the CD spectrum, after shaking, thermal equilibration, and subtraction of the Tris-HCl buffer. CD spectra in the range of 230−300 nm were analyzed.

DNA Intercalating Assay by Fluorescence Quenching. The fluorescence spectra were obtained using a Varian Cary Eclipse fluorescence spectrophotometer (1 cm quartz cell) at 25 °C. Two groups of samples were prepared with the concentration of compounds at 10, 20, 30, and 50 μM in Tris-HCl buffer (20 mM, pH 7.4): one contained 100 μM CT DNA, and the other contained no DNA as control. All of the above solution was incubated in the dark at 25 °C for 1 day. Fluorescence wavelength and intensity of the samples were recorded. The Scatchard binding constant was calculated.

DNA Relaxation Assay by Agarose Gel Electrophoresis. DNA relaxation was determined on 20 μL samples containing pBR322 (200 ng; Fermentas, Lithuania) and the target compounds (100 μM) in Tris-HCl buffer at pH 7.4. After incubation for 2 h at 37 °C, gel electrophoresis of the samples was performed using 1% agarose gel in TAB buffer. DNA was visualized by ethidium bromide (EB) staining for 20 min and photographed using a CHEMGENIUS 2 digital imaging system.

kDNA Decatenation Assay. The reaction mixture (20 μL) contained 4 μL of cleavage reaction buffer (50 mM Tris-HCl, pH

8.0, 120 mM KCl, 10 mM $MgCl_2$, 1 mM ATP, 0.5 mM DTT), 0.2 μg of kDNA, 0.2 μL of topo II (extract from HeLa cells), and 100 μM target compounds. After 15 min incubation at 37 °C, 10% SDS (2 μL) was added to the reaction mixture. Electrophoresis of the DNA samples was carried out in 1% agarose gel at 50 V/cm for 1 h. The gel was stained with 0.5 mg/mL EB and photographed using a CHEMGENIUS 2 digital imaging system.

Lysosomal Membrane Stability Assay. Untreated or treated with amonafide, **7a**−**d**, and **8a**−**d** at three concentrations respectively for 24 h, HeLa cells, both adherent and floating, were collected and stained with 20 μg/mL AO for 2 min at room temperature. Lysosomal membrane stability was determined by assessing AO red fluorescence with a flow cytometer (Becton Dickinson, USA).

Double Immunocytochemical Staining for Cytochrome *c*. HeLa cells were untreated or treated with **7a**−**d** and **8a**−**d** for 24 h at concentrations of 8, 3, 4, 4, 7, 6, 4, and 17 μM, respectively, corresponding their IC_{50} values. After being washed with PBS, cells were fixed with 10% formaldehyde at room temperature for 20 min, permeabilized with 90% methanol at −4 °C for 10 min, and blocked with 10% defatted milk at room temperature for 1 h. Cells were washed three times with PBS after fixation and permeabilization and with TBST after blocking. Next, cells were incubated with rabbit anti-cytochrome *c* (diluted 1:500; KeyGEN, Shanghai) for 1 h at room temperature and thereafter with FITC goat anti-rabbit IgG (diluted 1:100; KeyGEN, Shanghai) for 1 h at room temperature. Antibody was removed by washing three times with TBST, after each antibody incubation step. Finally, cells were counterstained with 2 μg/mL Hoechst 33258 for 30 min and then washed three times with TBST. Images were obtained using Nikon confocal laser scanning microscopy.

Annexin V-FIFC Apoptosis Detection Assay. After staining with annexin V-FITC and PI using the Annexin V-FITC apoptosis detection kit (Invitrogen, USA), cells were detected by flow cytometry to assess the membrane and nuclear events during apoptosis. Briefly, HeLa cells (1×10^6/1.5 mL per well) were seeded in six-well plates and treated with compounds **7a**−**d** and **8a**−**d** at concentrations of 8, 3, 4, 4, 7, 5, 4, and 16 μM, respectively, corresponding their IC_{50} values. After 24 h, cells were collected, washed twice with cold PBS, and resuspended in 400 μL of binding buffer which was then added to 5 μL of annexin V-FITC and incubated at 4 °C in the dark for 15 min. Subsequently, the buffer was added to 10 μL of PI and incubated at 4 °C in the dark for 5 min. The samples were analyzed by a FACScan flow cytometer (Becton Dickinson, USA).

Acknowledgment. This work was financially supported by the Key New Drug Creation and Manufacturing Program (2009ZX09103-102), the National High Technology Research and Development Program of China (863 Program 2006AA10A201), the China 111 Project (Grant B07023), and the Shanghai Leading Academic Discipline Project (B507).

References

(1) Sawyers, C. Targeted cancer therapy. *Nature* **2004**, *432* (7015), 294–297.
(2) Petrelli, A.; Giordano, S. From single- to multi-target drugs in cancer therapy: When aspecificity becomes an advantage. *Curr. Med. Chem.* **2008**, *15* (5), 422–432.
(3) Fu, Z.; Malureanu, L.; Huang, J.; Wang, W.; Li, H.; Van Deursen, J. M.; Tindall, D. J.; Chen, J. Plk1-dependent phosphorylation of FoxM1 regulates a transcriptional programme required for mitotic progression. *Nat. Cell Biol.* **2008**, *10* (9), 1076–1082.
(4) Overington, J. P.; Al-Lazikani, B.; Hopkins, A. L. Opinion—How many drug targets are there? *Nat. Rev. Drug Discov.* **2006**, *5* (12), 993–996.
(5) Szuromi, P.; Vinson, V.; Marshall, E. Rethinking drug discovery—Introduction. *Science* **2004**, *303* (5665), 1795–1795.
(6) Osterborg, A.; Mellstedt, H.; Keating, M. Clinical effects of alemtuzumab (Campath-1H) in B-cell chronic lymphocytic leukemia. *Med. Oncol.* **2002**, *19*, S21–S26.
(7) Bode, A. M.; Dong, Z. G. Cancer prevention research—Then and now. *Nat. Rev. Cancer* **2009**, *9* (7), 508–516.
(8) Zhan, P.; Liu, X. Y. Designed multiple ligands: An emerging anti-HIV drug discovery paradigm. *Curr. Pharm. Des.* **2009**, *15* (16), 1893–1917.
(9) Van der Schyf, C. J.; Geldenhuys, W. J. Polycyclic compounds: Ideal drug scaffolds for the design of multiple mechanism drugs? *Neurotherapeutics* **2009**, *6* (1), 175–186.
(10) Futerman, A. H.; Sussman, J. L.; Horowitz, M.; Silman, I.; Zimran, A. New directions in the treatment of Gaucher disease. *Trends Pharmacol. Sci.* **2004**, *25* (3), 147–151.
(11) Schrattenholz, A.; Soskic, V. What does systems biology mean for drug development? *Curr. Med. Chem.* **2008**, *15* (15), 1520–1528.
(12) Borisy, A. A.; Elliott, P. J.; Hurst, N. W.; Lee, M. S.; Lehar, J.; Price, E. R.; Serbedzija, G.; Zimmermann, G. R.; Foley, M. A.; Stockwell, B. R.; Keith, C. T. Systematic discovery of multicomponent therapeutics. *Proc. Natl. Acad. Sci. U.S.A.* **2003**, *100* (13), 7977–7982.
(13) Zimmermann, G. R.; Lehar, J.; Keith, C. T. Multi-target therapeutics: When the whole is greater than the sum of the parts. *Drug Discov. Today* **2007**, *12* (1−2), 34–42.
(14) Van der Greef, J.; McBurney, R. N. Innovation—Rescuing drug discovery: In vivo systems pathology and systems pharmacology. *Nat. Rev. Drug Discov.* **2005**, *4* (12), 961–967.
(15) Morphy, R.; Rankovic, Z. Designed multiple ligands. An emerging drug discovery paradigm. *J. Med. Chem.* **2005**, *48* (21), 6523–6543.
(16) Wei, D. G.; Jiang, X. L.; Zhou, L.; Chen, J.; Chen, Z.; He, C.; Yang, K.; Liu, Y.; Pei, J. F.; Lai, L. H. Discovery of multitarget inhibitors by combining molecular docking with common pharmacophore matching. *J. Med. Chem.* **2008**, *51* (24), 7882–7888.
(17) Hopkins, A. L. Network pharmacology: The next paradigm in drug discovery. *Nat. Chem. Biol.* **2008**, *4* (11), 682–690.
(18) Kerr, J. F. R.; Wyllie, A. H.; Currie, A. R. Apoptosis: A basic biological phenomenon with wide-ranging implications in tissue kinetics. *Br. J. Cancer* **1972**, *26* (4), 239–257.
(19) Fischer, U.; Janssen, K.; Schulze-Osthoff, K. Cutting-edge apoptosis-based therapeutics—A panacea for cancer? *Biodrugs* **2007**, *21* (5), 273–297.
(20) Thompson, C. B. Apoptosis in the pathogenesis and treatment of disease. *Science* **1995**, *267* (5203), 1456–1462.
(21) Reed, J. C. Apoptosis-based therapies. *Nat. Rev. Drug Discov.* **2002**, *1* (2), 111–121.
(22) Kroemer, G.; Galluzzi, L.; Brenner, C. Mitochondrial membrane permeabilization in cell death. *Physiol. Rev.* **2007**, *87* (1), 99–163.
(23) Tian, Z. Y.; Xie, S. Q.; Du, Y. W.; Ma, Y. F.; Zhao, J.; Gao, W. Y.; Wang, C. J. Synthesis, cytotoxicity and apoptosis of naphthalimide polyamine conjugates as antitumor agents. *Eur. J. Med. Chem.* **2009**, *44* (1), 393–399.
(24) Okada, H.; Mak, T. W. Pathways of apoptotic and non-apoptotic death in tumour cells. *Nat. Rev. Cancer* **2004**, *4* (8), 592–603.
(25) Fadeel, B.; Orrenius, S. Apoptosis: A basic biological phenomenon with wide-ranging implications in human disease. *J. Intern. Med.* **2005**, *258* (6), 479–517.
(26) Boya, P.; Kroemer, G. Lysosomal membrane permeabilization in cell death. *Oncogene* **2008**, *27* (50), 6434–6451.
(27) Hoyer-Hansen, M.; Jaattela, M. Autophagy—An emerging target for cancer therapy. *Autophagy* **2008**, *4* (5), 574–580.
(28) Gocheva, V.; Zeng, W.; Ke, D. X.; Klimstra, D.; Reinheckel, T.; Peters, C.; Hanahan, D.; Joyce, J. A. Distinct roles for cysteine cathepsin genes in multistage tumorigenesis. *Genes Dev.* **2006**, *20* (5), 543–556.
(29) Fehrenbacher, N.; Jaattela, M. Lysosomes as targets for cancer therapy. *Cancer Res.* **2005**, *65* (8), 2993–2995.
(30) Linder, S.; Shoshan, M. C. Lysosomes and endoplasmic reticulum: Targets for improved, selective anticancer therapy. *Drug Resist. Updates* **2005**, *8* (4), 199–204.
(31) Roy, D.; Liston, D. R.; Idone, V. J.; Di, A.; Nelson, D. J.; Pujol, C.; Bliska, J. B.; Chakrabarti, S.; Andrews, N. W. A process for controlling intracellular bacterial infections induced by membrane injury. *Science* **2004**, *304* (5676), 1515–1518.
(32) Kroemer, G.; Jaattela, M. Lysosomes and autophagy in cell death control. *Nat. Rev. Cancer* **2005**, *5* (11), 886–897.
(33) Erdal, H.; Berndtsson, M.; Castro, J.; Brunk, U.; Shoshan, M. C.; Linder, S. Induction of lysosomal membrane permeabilization by compounds that activate p53-independent apoptosis. *Proc. Natl. Acad. Sci. U.S.A.* **2005**, *102* (1), 192–197.
(34) Groth-Pedersen, L.; Ostenfeld, M. S.; Hoyer-Hansen, M.; Nylandsted, J.; Jaattela, M. Vincristine induces dramatic lysosomal changes and sensitizes cancer cells to lysosome-destabilizing siramesine. *Cancer Res.* **2007**, *67* (5), 2217–2225.
(35) Parry, M. J.; Alakoskela, J. M. I.; Khandelia, H.; Kumar, S. A.; Jaattela, M.; Mahalka, A. K.; Kinnunen, P. K. J. High-affinity

small molecule-phospholipid complex formation: Binding of siramesine to phosphatidic acid. *J. Am. Chem. Soc.* **2008**, *130* (39), 12953–12960.
(36) Ostenfeld, M. S.; Hoyer-Hansen, M.; Bastholm, L.; Fehrenbacher, N.; Olsen, O. D.; Groth-Pedersen, L.; Puustinen, P.; Kirkegaard-Sorensen, T.; Nylandsted, J.; Farkas, T.; Jaattela, M. Anti-cancer agent siramesine is a lysosomotropic detergent that induces cytoprotective autophagosome accumulation. *Autophagy* **2008**, *4* (4), 487–499.
(37) Li, W.; Yuan, X. M.; Nordgren, G.; Dalen, H.; Dubowchik, G. M.; Firestone, R. A.; Brunk, U. T. Induction of cell death by the lysosomotropic detergent MSDH. *FEBS Lett.* **2000**, *470* (1), 35–39.
(38) Ostenfeld, M. S.; Fehrenbacher, N.; Hoyer-Hansen, M.; Thomsen, C.; Farkas, T.; Jaattela, M. Effective tumor cell death by sigma-2 receptor ligand siramesine involves lysosomal leakage and oxidative stress. *Cancer Res.* **2005**, *65* (19), 8975–8983.
(39) Hurley, L. H. DNA and its associated processes as targets for cancer therapy. *Nat. Rev. Cancer* **2002**, *2* (3), 188–200.
(40) Tao, Z. F.; Wang, L.; Stewart, K. D.; Chen, Z. H.; Gu, W.; Bui, M. H.; Merta, P.; Zhang, H. Y.; Kovar, P.; Johnson, E.; Park, C.; Judge, R.; Rosenberg, S.; Sowin, T.; Lin, N. H. Structure-based design, synthesis, and biological evaluation of potent and selective macrocyclic checkpoint kinase 1 inhibitors. *J. Med. Chem.* **2007**, *50* (7), 1514–1527.
(41) Brana, M. F.; Ramos, A. Naphthalimides as anti-cancer agents: Synthesis and biological activity. *Curr. Med. Chem.: Anti-Cancer Agents* **2001**, *1* (3), 237–255.
(42) Ingrassia, L.; Lefranc, F.; Kiss, R.; Mijatovic, T. Naphthalimides and azonafides as promising anti-cancer agents. *Curr. Med. Chem.* **2009**, *16* (10), 1192–1213.
(43) Ratain, M. J.; Mick, R.; Berezin, F.; Janisch, L.; Schilsky, R. L.; Vogelzang, N. J.; Lane, L. B. Phase I study of amonafide dosing based on acetylator phenotype. *Cancer Res.* **1993**, *53* (10), 2304–2308.
(44) Brana, M. F.; Cacho, M.; Garcia, M. A.; de Pascual-Teresa, B.; Ramos, A.; Dominguez, M. T.; Pozuelo, J. M.; Abradelo, C.; Rey-Stolle, M. F.; Yuste, M.; Banez-Coronel, M.; Lacal, J. C. New analogues of amonafide and elinafide, containing aromatic heterocycles: Synthesis, antitumor activity, molecular modeling, and DNA binding properties. *J. Med. Chem.* **2004**, *47* (6), 1391–1399.
(45) Antonini, I.; Santoni, G.; Lucciarini, R.; Amantini, C.; Sparapani, S.; Magnano, A. Synthesis and biological evaluation of new asymmetrical bisintercalators as potential antitumor drugs. *J. Med. Chem.* **2006**, *49* (24), 7198–7207.
(46) Van Quaquebeke, E.; Mahieu, T.; Dumont, P.; Dewelle, J.; Ribaucour, F.; Simon, G.; Sauvage, S.; Gaussin, J. F.; Tuti, J.; El Yazidi, M.; Van Vynckt, F.; Mijatovic, T.; Lefranc, F.; Darro, F.; Kiss, R. 2,2,2-Trichloro-N-({2-[2-(dimethylamino)ethyl]-1,3-dioxo- 2,3-dihydro-1H-benzo[de]isoquinolin5-yl}carbamoyl)acetamide (UNBS3157), a novel nonhematotoxic naphthalimide derivative with potent antitumor activity. *J. Med. Chem.* **2007**, *50* (17), 4122–4134.
(47) Tumiatti, V.; Milelli, A.; Minarini, A.; Rosini, M.; Bolognesi, M. L.; Micco, M.; Andrisano, V.; Bartolini, M.; Mancini, F.; Recanatini, M.; Cavalli, A.; Melchiorre, C. Structure-activity relationships of acetylcholinesterase noncovalent inhibitors based on a polyamine backbone. 4. Further investigation on the inner spacer. *J. Med. Chem.* **2008**, *51* (22), 7308–7312.
(48) Li, Z. G.; Yang, Q.; Qian, X. H. Novel thiazonaphthalimides as efficient antitumor and DNA photocleaving agents: Effects of intercalation, side chains, and substituent groups. *Biorg. Med. Chem.* **2005**, *13* (16), 4864–4870.
(49) Norton, J. T.; Witsch, M. A.; Luong, L.; Kawamura, A.; Ghosh, S.; Stack, M. S.; Sim, E.; Avram, M. J.; Appella, D. H.; Huang, S. Synthesis and anticancer activities of 6-amino amonafide derivatives. *Anti-Cancer Drugs* **2008**, *19* (1), 23–36.
(50) Iranpoor, N.; Firouzabadi, H.; Aghapour, G.; Vaezzadeh, A. R. Triphenylphosphine/2,3-dichloro-5,6-dicyanobenzoquinone as a new, selective and neutral system for the facile conversion of alcohols, thiols and selenols to alkyl halides in the presence of halide ions. *Tetrahedron* **2002**, *58* (43), 8689–8693.
(51) Xuhong, Q.; Zhenghua, Z.; Kongchang, C. A study on the Ullmann condensation reaction of 4-chloro-1,8-naphthalic anhydride with N,N-dimethylformamide. *J. Prakt. Chem./Chem.-Ztg.* **1992**, *334* (2), 161–164.
(52) Ott, I.; Xu, Y. F.; Liu, J. W.; Kokoschka, M.; Harlos, M.; Sheldrick, W. S.; Qian, X. H. Sulfur-substituted naphthalimides as photoactivatable anticancer agents: DNA interaction, fluorescence imaging, and phototoxic effects in cultured tumor cells. *Biorg. Med. Chem.* **2008**, *16* (15), 7107–7116.
(53) Zhang, Z. C.; Yang, Y. Y.; Zhang, D. N.; Wang, Y. Y.; Qian, X. H.; Liu, F. Y. Acenaphtho[1,2-b]pyrrole derivatives as new family of intercalators: Various DNA binding geometry and interesting antitumor capacity. *Biorg. Med. Chem.* **2006**, *14* (20), 6962–6970.
(54) Mizushima, T.; Natori, S.; Sekimizu, K. Relaxation of supercoiled DNA associated with induction of heat shock proteins in *Escherichia coli*. *Mol. Gen. Genet.* **1993**, *238* (1−2), 1–5.
(55) Wang, J. C. Cellular roles of DNA topoisomerases: A molecular perspective. *Nat. Rev. Mol. Cell Biol.* **2002**, *3* (6), 430–440.
(56) Li, T. K.; Liu, L. F. Tumor cell death induced by topoisomerase-targeting drugs. *Annu. Rev. Pharmacol. Toxicol.* **2001**, *41*, 53–77.
(57) Larsen, A. K.; Escargueil, A. E.; Skladanowski, A. Catalytic topoisomerase II inhibitors in cancer therapy. *Pharmacol. Ther.* **2003**, *99* (2), 167–181.
(58) Zhu, H.; Huang, M.; Yang, F.; Chen, Y.; Miao, Z. H.; Qian, X. H.; Xu, Y. F.; Qin, Y. X.; Luo, H. B.; Shen, X.; Geng, M. Y.; Cai, Y. J.; Ding, J. R16, a novel amonafide analogue, induces apoptosis and G(2)-M arrest via poisoning topoisomerase II. *Mol. Cancer Ther.* **2007**, *6* (2), 484–495.
(59) Tanabe, K.; Ikegami, Y.; Ishida, R.; Andoh, T. Inhibition of topoisomerase-II by antitumor agents bis(2,6-dioxopiperazine) derivatives. *Cancer Res.* **1991**, *51* (18), 4903–4908.
(60) Zdolsek, J. M.; Olsson, G. M.; Brunk, U. T. Photooxidative damage to lysosomes of cultured macrophages by acridine orange. *Photochem. Photobiol.* **1990**, *51* (1), 67–76.
(61) Boya, P.; Andreau, K.; Poncet, D.; Zamzami, N.; Perfettini, J. L.; Metivier, D.; Ojcius, D. M.; Jaattela, M.; Kroemer, G. Lysosomal membrane permeabilization induces cell death in a mitochondrion-dependent fashion. *J. Exp. Med.* **2003**, *197* (10), 1323–1334.
(62) Yuan, X. M.; Li, W.; Dalen, H.; Lotem, J.; Kama, R.; Sachs, L.; Brunk, U. T. Lysosomal destabilization in p53-induced apoptosis. *Proc. Natl. Acad. Sci. U.S.A.* **2002**, *99* (9), 6286–6291.
(63) Green, D. R.; Reed, J. C. Mitochondria and apoptosis. *Science* **1998**, *281* (5381), 1309–1312.
(64) Garrido, C.; Galluzzi, L.; Brunet, M.; Puig, P. E.; Didelot, C.; Kroemer, G. Mechanisms of cytochrome *c* release from mitochondria. *Cell Death Differ.* **2006**, *13* (9), 1423–1433.
(65) Lim, M. L. R.; Chen, B. H.; Beart, P. M.; Nagley, P. Relative timing of redistribution of cytochrome *c* and Smac/DIABLO from mitochondria during apoptosis assessed by double immunocytochemistry on mammalian cells. *Exp. Cell Res.* **2006**, *312* (7), 1174–1184.
(66) Vermes, I.; Haanen, C.; Steffensnakken, H.; Reutelingsperger, C. A novel assay for apoptosis. Flow cytometric detection of phosphatidylserine expression on early apoptotic cells using fluorescein labeled Annexin V. *J. Immunol. Methods* **1995**, *184* (1), 39–51.
(67) Riccardi, C.; Nicoletti, I. Analysis of apoptosis by propidium iodide staining and flow cytometry. *Nat. Protoc.* **2006**, *1*, 1458–1461.
(68) Zhang, W. T.; Ruan, J. L.; Wu, P. F.; Jiang, F. C.; Zhang, L. N.; Fang, W.; Chen, X. L.; Wang, Y.; Cao, B. S.; Chen, G. Y.; Zhu, Y. J.; Gu, J.; Chen, J. G. Design, synthesis, and cytoprotective effect of 2-aminothiazole analogues as potent poly(ADP-ribose) polymerase-1 inhibitors. *J. Med. Chem.* **2009**, *52* (3), 718–725.
(69) Joo, S. S.; Yoo, Y. M. Melatonin induces apoptotic death in LNCaP cells via p38 and JNK pathways: Therapeutic implications for prostate cancer. *J. Pineal Res.* **2009**, *47* (1), 8–14.